INSTITUTE OF PHYSICS PUBLISHING JOURNAL OF PHYSICS: CONDENSED MATTER

J. Phys.: Condens. Matter **14** (2002) 3705–3713 PII: S0953-8984(02)31892-7

Liquid crystalline states in quantum Hall systems

Carlos Wexler and Orion Ciftja

Department of Physics and Astronomy, University of Missouri-Columbia, Columbia, MO 65211, USA

E-mail: wexlerc@missouri.edu and ciftjao@missouri.edu

Received 14 December 2001
Published 28 March 2002
Online at stacks.iop.org/JPhysCM/14/3705

Abstract

We investigate liquid crystalline phases with nematic order at $\frac{1}{3}$-filling of the valence Landau level (LL). We generalize Laughlin's fractional quantum Hall (QH) effect wavefunction at $\nu = \frac{1}{3}$ to include anisotropic nodal distribution by modifying the Jastrow factors. Lengthy Monte Carlo simulations are then used to determine with unprecedented accuracy the (anisotropic) pair distribution function $g(\boldsymbol{r})$ and static structure factor $S(\boldsymbol{q})$ for various degrees of anisotropy. The determination of the correlation energies at $\frac{1}{3}$-filling of an arbitrary LL is then performed by using standard mappings of $g(\boldsymbol{r})$ and $S(\boldsymbol{q})$ to higher LLs. Our results indicate that while Laughlin's state is stable in the lowest LL, there are regions of instability towards nematic order in higher LLs. Possible connections to the recently discovered QH liquid crystals are discussed.

1. Introduction

There has been renewed interest in the many-body physics of two-dimensional electron systems (2DES) in a strong perpendicular magnetic field, when the topmost or valence Landau level (LL) is partially filled. Because of the quenching of the kinetic energy, the tremendous mobilities achievable in the interfacial region of state-of-the-art GaAs/$Al_xGa_{1-x}As$ heterostructures, and the relative enhancement of interactions due to the reduced dimensionality, subtle electronic correlations are readily observable and new phases become evident as sample quality improves and temperatures are lowered. It is quite remarkable that over the last 20 years, 2DES have become one of the most important benchmarks in both experimental and theoretical physics, generating an extraordinary number of important new ideas [1], such as: the existence of fractionally charged quasiparticles [2], topological quantum numbers [3], chiral Luttinger liquids [4], and composite particles [5].

Recently, a number of unexpected phenomena were observed in the transitional regions between different plateaus of the Hall conductance of LLs with index $L \geqslant 2$: near half-filling of the valence LL, extreme anisotropy has been measured in the magnetotransport

below temperatures of about 100 mK [6–8], accompanied by smooth non-linearities of the conductance [6]. In addition, re-entrant integer quantum Hall effect (RIQHE) regions with striking breakdown features and new phase transitions (presumed to be quantum in origin [9]) have been seen near $\frac{1}{4}$-filling of the valence LL [10]. The anisotropic behaviour has been attributed to the formation of a nematic phase of the 2DES which then undergoes a nematic-to-isotropic transition at higher temperatures [9,11]. Similarly, the re-entrant regions are believed to be 'bubble phases' similar to Wigner crystals, but with several electrons per bubble, or possibly new electronic hexatic states [9].

The aim of our work is to study these numerous liquid crystalline phases present in partially filled LLs by means of many-body trial wavefunctions with a nematic symmetry. Previously we reported on approximate hypernetted chain (HNC) methods used to consider similar broken-rotational-symmetry (BRS) states at $\frac{1}{3}$-filling [12] and $\frac{1}{2}$-filling [13] of a LL, where we found that isotropic states (Laughlin for $\nu = \frac{1}{3}$, Rezayi–Read for $\nu = \frac{1}{2}$) are stable in the lowest Landau level (LLL), but BRS states were favourable for $L \geqslant 1$. Whereas these results are indeed compelling, it is highly desirable to obtain independent verification of these conclusions by alternate means, considering the approximate nature of the HNC, the small size of the energy differences obtained, and the fact that Musaelian and Joynt (MJ) had previously conjectured that BRS states could be possible at $\nu = \frac{1}{3}$ (in the LLL) [14]. In this paper we present an essentially exact Monte Carlo (MC) determination of the optimal phase (isotropic versus nematic) for a 2DES with a $\frac{1}{3}$-filled topmost LL described by a generalized MJ [14] wavefunction of the form

$$\Psi_\alpha(\boldsymbol{r}_1, \ldots, \boldsymbol{r}_N) = \prod_{i<j}^{N} (z_i - z_j)(z_i - z_j - \alpha)(z_i - z_j + \alpha) \exp\left(-\tfrac{1}{4} \sum_{k=1}^{N} |z_k|^2\right), \tag{1}$$

where $z_j = x_j + \mathrm{i}y_j$ is the complex 2D coordinate of the jth electron and α is a complex number (we work in units of the magnetic length: $l_0^2 = \hbar/eB = 1$). This wavefunction represents a homogeneous liquid state with filling factor $\nu = \frac{1}{3}$, lies entirely in the LLL (below we describe the generalization to higher LLs), and for $\alpha \neq 0$ has nematic order (for $\alpha = 0$ we recover Laughlin's wavefunction [2], which is obviously isotropic). This wavefunction represents, therefore, a good starting point for considering nematic QH systems. Note, however, that QH nematics were observed for $\frac{1}{2}$-fillings rather than $\frac{1}{3}$-fillings of the valence LLs. Fermi HNC analysis [13] of the $\frac{1}{2}$-filling case shows considerable similarities to the latter case, while extensive and extremely time-consuming MC simulations are currently being undertaken [15]. The availability of MC and HNC methods for both filling factors is, in any case, quite desirable for a direct comparison and for a systematic study of the energy dependence of BRS states for diverse physical parameters (LL index, width of the 2DES, etc). In addition, the possibility of BRS states for $\nu = \frac{1}{3}$ is intriguing in itself, since for $\alpha \neq 0$ highly damped low-energy modes exist [11,16], strongly modifying the dynamics and possibly suppressing the fractional quantum Hall effect (FQHE).

In order to determine the optimal electronic configuration (using the anisotropy-generating parameter α variationally), we calculated the correlation energies for families of states described by equation (1) by averaging over billions of MC-generated configurations. Eighty to 800 electrons were used in the MC runs and the results were extrapolated to the thermodynamic limit. To a very high degree of confidence, we find that Laughlin's state (isotropic: $\alpha = 0$) is favourable in the lowest and first excited LLs for all sample widths probed in [12] (LLL only) and [14], in partial agreement with our previous HNC results [12]. At higher LLs BRS states are favourable for a wide range of sample widths, in good agreement with our HNC results [12].

In section 2 we present the basic theoretical calculations needed to determine the stability of an isotropic or BRS state. In section 3 we briefly discuss the MC method used in the context of the BRS wavefunction (equation (1)). The results for the BRS state in the LLL and their extension to higher LLs are discussed in section 4.

2. Basic theory

In this work we propose to study the stability of different states by using trial wavefunctions of the form of equation (1). We perform this analysis by comparing the energy in each of these states to find the optimum value for the anisotropy-generating parameter α.

We first consider the situation in the LLL, namely the state with $\nu = \frac{1}{3}$. Since the BRS wavefunction is completely in the LLL, the kinetic energy per particle is quenched at the lowest cyclotron energy:

$$\frac{1}{N}\frac{\langle\Psi_\alpha|\hat{K}|\Psi_\alpha\rangle}{\langle\Psi_\alpha|\Psi_\alpha\rangle} = \frac{1}{2}\hbar\omega_c, \tag{2}$$

where $\omega_c = eB/m$ is the cyclotron frequency (for higher LLs, the kinetic energy is still quenched, albeit at a higher value). The potential, or correlation energy per electron is

$$E_\alpha = \frac{1}{N}\frac{\langle\Psi_\alpha|\hat{V}|\Psi_\alpha\rangle}{\langle\Psi_\alpha|\Psi_\alpha\rangle}, \tag{3}$$

where $\hat{V}$ represents the electron–electron, electron–background, and background–background interaction. While this quantity can be computed directly using standard MC sampling (section 3), a new MC run has to be performed if the potential V needs to be changed (e.g. by considering a different sample width in the third dimension, or a particular screening length). In addition, a new MC sampling would also be needed for each LL (and the correlated many-body wavefunction is quite cumbersome). Fortunately, for two-body potentials, this correlation energy may also be written as

$$E_\alpha = \frac{\rho}{2}\int \mathrm{d}^2 r\, V(r)[g(\boldsymbol{r}) - 1], \tag{4}$$

where $g(\boldsymbol{r})$ is the (angle-dependent) pair distribution function given by

$$g(\boldsymbol{r}) = \frac{N(N-1)}{\rho^2}\frac{\int \mathrm{d}^2 r_3 \cdots \mathrm{d}^2 r_N\, |\Psi_\alpha(\boldsymbol{r}_1, \ldots, \boldsymbol{r}_N)|^2}{\int \mathrm{d}^2 r_1 \cdots \mathrm{d}^2 r_N\, |\Psi_\alpha(\boldsymbol{r}_1, \ldots, \boldsymbol{r}_N)|^2}, \tag{5}$$

where $\boldsymbol{r} = \boldsymbol{r}_2 - \boldsymbol{r}_1$, and which satisfies the *normalization condition*: $\rho \int \mathrm{d}^2 r\, [g(\boldsymbol{r}) - 1] = -1$. For an ideal 2D sample the interaction is a pure Coulomb potential $V(r) \simeq e^2/(\epsilon r)$, while in samples with finite thickness a reasonable choice is the Zhang–Das Sarma (ZDS) potential $V(r) = e^2/(\epsilon\sqrt{r^2 + \lambda^2})$ [17], where λ is of the order of the sample thickness. Alternatively, the correlation energy can be computed in reciprocal space:

$$E_\alpha = \frac{1}{2}\int \frac{\mathrm{d}^2 q}{(2\pi)^2}\, \tilde{V}(q)[S(\boldsymbol{q}) - 1], \tag{6}$$

where $\tilde{V}(q)$ is the 2D Fourier transform (FT) of $V(r)$:

$$\tilde{V}(q) = \int \mathrm{d}^2 r\, \mathrm{e}^{-\mathrm{i}\boldsymbol{q}\cdot\boldsymbol{r}} V(r) = 2\pi \int_0^\infty \mathrm{d}r\, r J_0(qr) V(r), \tag{7}$$

and the static structure factor $S(\boldsymbol{q})$ is related by FT to $g(\boldsymbol{r})$:

$$S(\boldsymbol{q}) - 1 = \rho \int \mathrm{d}^2 r\, \mathrm{e}^{-\mathrm{i}\boldsymbol{q}\cdot\boldsymbol{r}}[g(\boldsymbol{r}) - 1]. \tag{8}$$

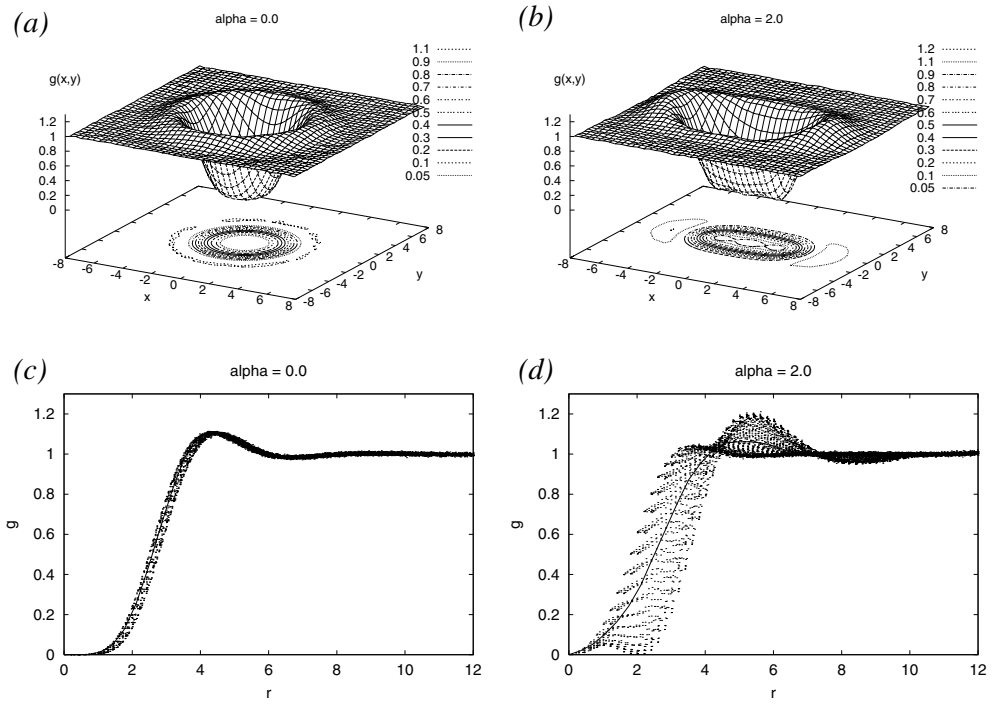

Figure 1. The pair distribution function at $\nu = 1/3$: (*a*) and (*b*) ($\alpha = 0, 2$ respectively): surface and contour plots of $g(\boldsymbol{r})$; (*c*) and (*d*) ($\alpha = 0, 2$ respectively): dotted curves: $g(r, \theta)$ for various $\theta \in [0, 2\pi]$; full curve: angle-averaged $\overline{g}(r)$; note the discrete nodes of $g(r, \theta)$ at $r = \alpha, \theta = \theta_\alpha, \theta_\alpha + \pi$ ($\theta_\alpha = 0$ in this case). For the plots above, 10^{10} MC steps were performed for each α on 200 electrons.

Although $g(\boldsymbol{r})$ and $S(\boldsymbol{q})$ are both angle dependent (e.g. see figures 1 and 2), since the interaction potential is centrally symmetric, the energy E_α depends only on the angle-averaged pair distribution function or static structure factor defined as

$$\overline{g}(r) = \int_0^{2\pi} \frac{\mathrm{d}\theta}{2\pi}\, g(\boldsymbol{r}), \qquad \overline{S}(q) = \int_0^{2\pi} \frac{\mathrm{d}\theta_q}{2\pi}\, S(\boldsymbol{q}). \tag{9}$$

The determination of either the pair distribution function or the static structure factor can be readily computed by MC simulation (section 3), but generally this is a time-consuming process that needs to be performed for each LL. However, it is known that if transitions to other LLs are neglected (i.e. a *single-LL approximation*), $g(\boldsymbol{r})$ and $S(\boldsymbol{q})$ at higher LL are simply related to those at the LLL ($L = 0$) by means of a convolution or product respectively. We will apply this approximation (which, moreover, quenches the kinetic energy in higher LLs as well). It is then sufficient to compute these distribution functions only in the LLL and then the correlation energy per electron in an arbitrary LL with index L is given by

$$E_\alpha^L = \frac{1}{2} \int \frac{\mathrm{d}^2 q}{(2\pi)^2}\, \tilde{V}_{\mathrm{eff}}(q)[S(\boldsymbol{q}) - 1], \tag{10}$$

where $\tilde{V}_{\mathrm{eff}}(q) \equiv \tilde{V}(q)[L_L(q^2/2)]^2$, $L_L(x)$ are Laguerre polynomials, and $S(\boldsymbol{q})$ is calculated in the LLL ($L = 0$).

In what follows we compute $g(\boldsymbol{r})$ and $S(\boldsymbol{q})$ through MC simulations with a probability distribution given by $|\Psi_\alpha(\boldsymbol{r}_1, \ldots, \boldsymbol{r}_N)|^2$ (equation (1)).

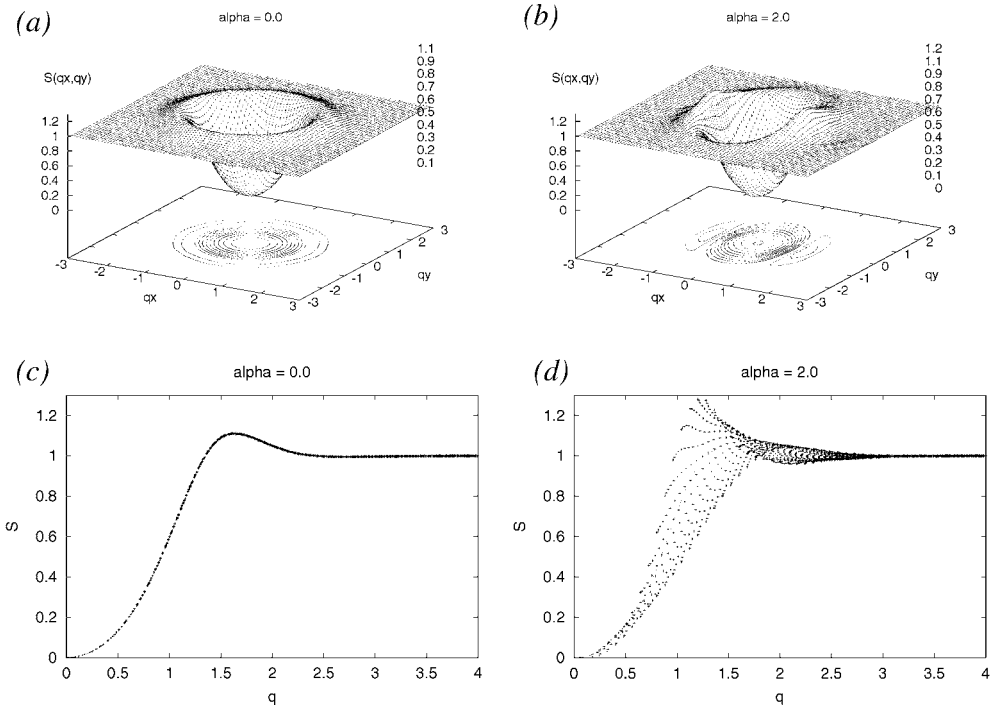

Figure 2. The static structure factor at $\nu = 1/3$: (*a*) and (*b*) ($\alpha = 0, 2$ respectively): surface and contour plots of $S(\boldsymbol{q})$; (*c*) and (*d*) ($\alpha = 0, 2$ respectively): dotted curves: $S(q, \theta_q)$ for various $\theta_q \in [0, 2\pi]$; full curve: angle-averaged $\overline{S}(q)$; note, for $\alpha \neq 0$, the presence of directional peaks in $S(\boldsymbol{q})$ consistent with a nematic structure. The static structure factors were calculated from the pair distribution functions (see figure 1) using equation (8).

3. Monte Carlo determination of the pair correlation function, static structure factor, and correlation energy

In order to determine the pair distribution function $g(\boldsymbol{r})$, we perform standard Metropolis MC [18] simulations of the 2DES on a plane with a probability distribution given by

$$\begin{aligned} P(\boldsymbol{r}_1, \ldots, \boldsymbol{r}_N) &\equiv |\Psi_\alpha(\boldsymbol{r}_1, \ldots, \boldsymbol{r}_N)|^2 \\ &= \prod_{i<j}^{N} |(z_i - z_j)(z_i - z_j - \alpha)(z_i - z_j + \alpha)|^2 \exp\left(-\tfrac{1}{2}\sum_{k=i}^{N} |z_k|^2\right) \\ &= \exp\left[\sum_{i<j}^{N} \log(\boldsymbol{r}_i - \boldsymbol{r}_j)^2 + \log(\boldsymbol{r}_i - \boldsymbol{r}_j - \boldsymbol{\alpha})^2 + \log(\boldsymbol{r}_i - \boldsymbol{r}_j + \boldsymbol{\alpha})^2 - \sum_{k=1}^{N} \frac{r_k^2}{2}\right], \end{aligned} \tag{11}$$

where we omitted irrelevant normalization constants.

For each α under consideration, we start by uniformly distributing N electrons inside a disc of radius $R \simeq \sqrt{2N/\nu}$. In each MC step, a random electron is moved a fixed distance d (chosen at the beginning of the run so that approximately 50% of the MC attempts are successful) in a random angle. Using the standard Metropolis algorithm [18], we accept the move if $P^{\text{new}}/P^{\text{old}}$ is bigger than a random number between 0 and 1, and otherwise reject it. After an initial 'thermalization' process of several million MC steps, we compute $g(\boldsymbol{r})$

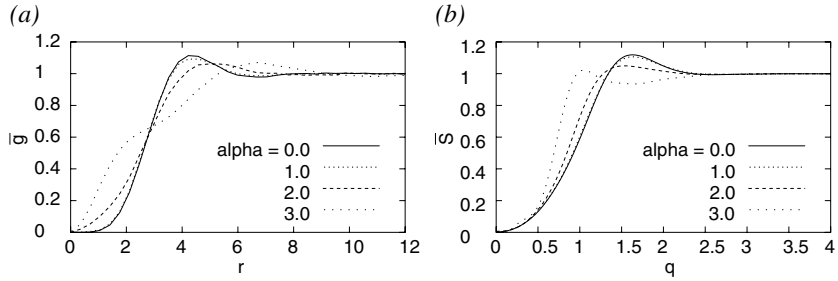

Figure 3. The angle-averaged pair distribution function $\overline{g}(r)$ (panel (*a*)) and static structure factor $\overline{S}(q)$ (panel (*b*)).

by counting how many electrons are present in a discrete Cartesian array centred around each *other* electron; this counting process is averaged over several billion MC steps requiring several hours to a few days of computation on a state-of-the-art Alpha 21 264 workstation. Eighty to 800 electrons were used in the MC runs and the results were extrapolated to the thermodynamic limit. Care is taken so that only electrons in the 'bulk' of this system are counted (by excluding a ring near the periphery of the disk). Direct calculations of the correlation energy in the LLL for various potentials were also performed to further verify our results.

4. Results and discussion

In this work we applied MC methods to study BRS states at a $\frac{1}{3}$-filling of an arbitrary LL (in the single-LL approximation). Extensive MC simulations in the disc geometry have allowed us to determine to a very good accuracy the pair distribution function and the static structure factor. In order to compare the isotropic (Laughlin's, $\alpha = 0$) state with the BRS states ($\alpha \neq 0$) we studies their properties for various αs with magnitudes between 0 and 3 (in general $\alpha = |\alpha|e^{i\theta_\alpha}$; we considered $\theta_\alpha = 0$ without loss of generality).

In figure 1 we plot the pair distribution function $g(\boldsymbol{r})$ for $\alpha = 0$ and 2. It is interesting to note, for $\alpha \neq 0$, the noticeable angle dependence of $g(\boldsymbol{r})$, and the splitting of the triple node at the origin to a simple node at the origin and additional simple nodes at $r = \alpha$ and angle $\theta = \theta_\alpha, \theta_\alpha + \pi$ ($\theta_\alpha = 0$ in this case). Figure 2 shows the static structure factor $S(\boldsymbol{q})$ for $\alpha = 0$ and 2, calculated from $g(\boldsymbol{r})$ by means of the FT defined in equation (8). Note for $\alpha \neq 0$ the presence of directional peaks in $S(\boldsymbol{q})$ consistent with a nematic order.

Due to the rotational symmetry of the interaction potential, from the energetics point of view (see equations (4), (10) and (9)), the dependence of the angle-averaged $\overline{g}(r)$ and $\overline{S}(q)$ is a major consideration. Figure 3 shows the angle-averaged pair distribution function and structure factor for $\alpha = 0$, 1, 2, and 3. As α is increased the major peak of $\overline{g}(r)$ becomes less pronounced and shifts towards higher radii, and simultaneously a shoulder develops and becomes clearly visible near $r = 2$ for $\alpha = 3$; finally the small-r behaviour shifts from $\overline{g}(r) \propto r^6$ (for $\alpha = 0$) to r^2 for $\alpha \neq 0$. The dependence of $\overline{S}(q)$ on α is also quite noticeable: as it is increased the peak narrows and shifts towards smaller q, but there is no change in the small-q behaviour.

One can compute the correlation energy per particle directly from equations (4), (6), or (10) to determine the energy per electron for arbitrary values of the BRS parameter α, the

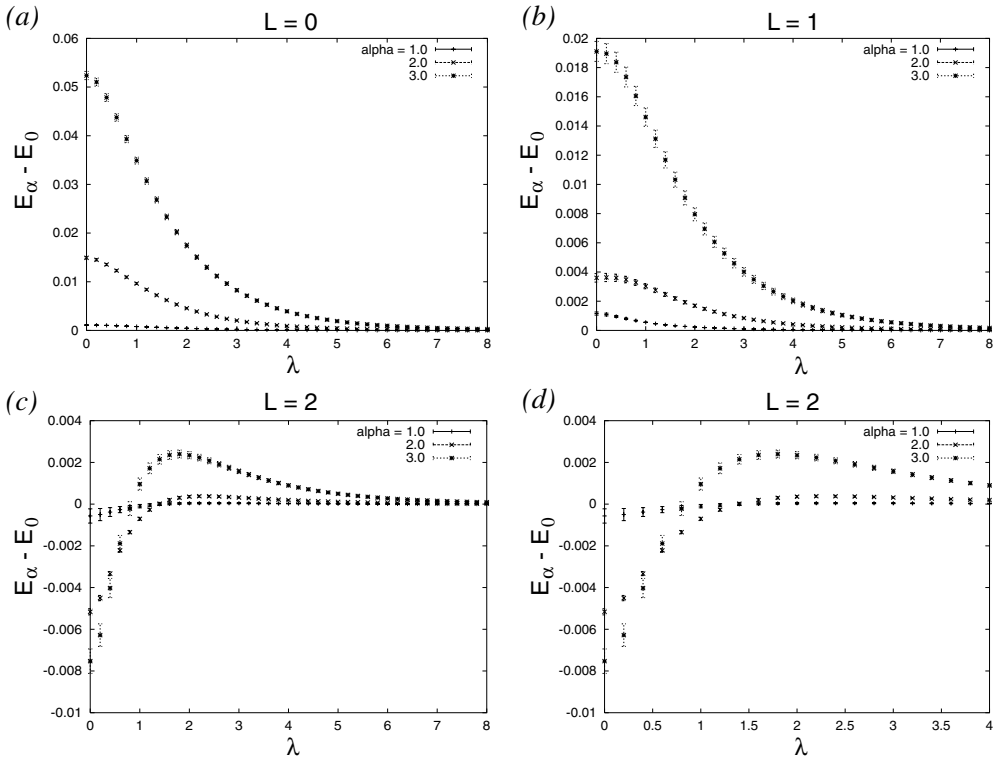

Figure 4. Correlation energy per particle in BRS states with $\alpha = 1$, 2, and 3 relative to the isotropic ($\alpha = 0$) state for various Landau levels L as a function of the short-distance cut-off λ (see the comments preceding equation (6), and [17]). The energies are in units of $e^2/(\epsilon l_0)$. (*a*) LLL ($L = 0$); (*b*) first excited LL ($L = 1$); (*c*) second excited LL ($L = 2$); (*d*) detail of (*c*). Note that there are ranges of λ for which BRS states are favourable for the last case ($L = 2$).

2D system width λ, and LL index L. The following simplified formula can be used, in view of equation (9):

$$E_\alpha^L(\lambda) = \frac{1}{4\pi}\int_0^\infty \mathrm{d}q\, q\tilde{V}(q,\lambda)\left[L_L\left(\frac{q^2}{2}\right)\right]^2[\overline{S}(q)-1], \tag{12}$$

where $\tilde{V}(q,\lambda) = (2\pi e^2/\epsilon q)\exp(-\lambda q)$ is the 2D FT of the ZDS interaction potential [17]. This allows straightforward calculations to be extended to any LL.

Figure 4 shows the energy difference between BRS states with $\alpha = 1$, 2, and 3, and the isotropic state with $\alpha = 0$. Our findings indicate that in the LLL ($L = 0$) the isotropic Laughlin state is stable for all λ that we considered, since all $\alpha \neq 0$ states have higher energies (top panel). This results are in significant disagreement with those of [14] and coincide *quantitatively* with our previous HNC calculations [12]. We also observe stability of the isotropic state in the first excited LL[1] ($L = 1$, $\nu = 2 + \frac{1}{3}$). The situation changes considerably in the second excited

[1] Our previous HNC calculation [12] predicted a BRS instability for $L = 1$. MC results should be, however, preferred, given the approximate nature of the HNC methods. Note that for each LL there are two spin sub-bands. The case under consideration ($\frac{1}{3}$-filling of the valence LL) therefore allows $\nu = \frac{1}{3}$ and $\nu = 1 + \frac{1}{3}$ in the LLL ($L = 0$), $\nu = 2 + \frac{1}{3}$ and $\nu = 3 + \frac{1}{3}$ for $L = 1$, etc. For simplicity we only *explicitly* consider partial fillings of the lower spin sub-band, but most of the results can be readily applied to the upper sub-band as well.

LLs ($L = 2$, $\nu = 4 + \frac{1}{3}$ (see footnote 1)) where, for a considerable range of the short-distance cut-off λ, BRS states are found to have *lower* energies and the incompressible Laughlin-like state is unstable towards a nematic state (see lower panels of figure 4), also in agreement with [12].

At this point it is important to comment on how precise our determination of the energy differences is. The only significant sources of error in our calculations arise from the statistical errors due to finite sampling and the discrete nature of the grid used in the determination of the pair distribution function $g(\boldsymbol{r})$ (these errors are inherent to all MC methods). The errors propagate to the static structure factor $S(\boldsymbol{q})$, and are amplified at large q by the Laguerre polynomials in equation (10). The error bars in figure 4 are estimated by comparing our $\overline{S}(q)$ to analytical approximations calculated (for the isotropic state) by Girvin *et al* [19].

5. Conclusions

In conclusion, we have applied MC methods to study possible BRS states for $\frac{1}{3}$-filling of an arbitrary LL. We find that the isotropic Laughlin-like state is stable for the lowest ($L = 0$) and first excited ($L = 1$) LL, whereas a BRS instability is possible in the second excited ($L = 2$) LL. Since BRS states are gapless and heavily damped [11, 16] this may offer a simple explanation for the absence of the FQHE in higher LLs. While these results are quite interesting and compelling, the connection to recent observations of liquid crystalline states [6–11] in half- and quarter-filled LLs requires a more sophisticated treatment. One possibility is to use anisotropic generalizations of the Rezayi–Read wavefunction [20] valid for a $\frac{1}{2}$-filled LL:

$$\Psi_\alpha(\boldsymbol{r}_1, \ldots, \boldsymbol{r}_N) = \hat{P}_L \prod_{j<k}^{N} (z_j - z_k + \alpha)(z_j - z_k - \alpha) \exp\left(- \sum_{k=1}^{N} |z_k|^2/4 \right) \det[\varphi_k(\boldsymbol{r}_i)], \quad (13)$$

where $\hat{P}_L$ represents a projector onto the Lth LL. In [13] we explored such states using the Fermi HNC approximation and found similar results. A verification of these results using the more accurate MC procedures of this paper using a probability distribution derived from equation (13) is currently under way [15].

Acknowledgments

We would like to acknowledge helpful discussions with A J Schmidt, A T Dorsey, M Fogler and L Radzihovsky. This work was supported by the University of Missouri Research Board.

References

[1] Das Sarma S and Pinczuk A (ed) 1996 *Perspectives in Quantum Hall Effects* (New York: Wiley)
[2] Laughlin R B 1983 *Phys. Rev. Lett.* **50** 1395
[3] Thouless D J 1998 *Topological Quantum Numbers in Nonrelativistic Physics* (Singapore: World Scientific)
[4] Wen X G 1991 *Phys. Rev.* B **43** 11 025
Wen X G 1990 *Phys. Rev. Lett.* **64** 2206
[5] For a review see: Jain J 2000 The composite fermion: a quantum particle and its quantum fluids *Phys. Today* (4) 39
Heinonen O (ed) *Composite Fermions* (New York: World Scientific)
[6] Lilly M P, Cooper K B, Eisenstein J P, Pfeiffer L N and West K W 1999 *Phys. Rev. Lett.* **82** 394
[7] Du R R, Tsui D C, Stormer H L, Pfeiffer L N, Baldwin K W and West K W 1999 *Solid State Commun.* **109** 389
[8] Shayegan M, Manoharan H C, Papadakis S J and DePoortere E P 2000 *Physica* E **6** 40

[9] Fradkin E and Kivelson S A 1999 *Phys. Rev.* B **59** 8065
[10] Cooper K B, Lilly M P, Eisenstein J P, Pfeiffer L N and West K W 1999 *Phys. Rev.* B **60** 11 285
[11] Wexler C and Dorsey A T 2001 *Phys. Rev.* B **64** 115312
[12] Ciftja O and Wexler C 2002 *Phys. Rev.* B **65** 045306
[13] Ciftja O and Wexler C 2001 *Phys. Rev.* B at press (cond-mat/0111120)
[14] Musaelian K and Joynt R 1996 *J. Phys.: Condens. Matter* **8** L105
[15] Schmidt A J, Ciftja O and Wexler C 2002 in preparation
[16] Fogler M M and Vinokur V M 2000 *Phys. Rev. Lett.* **84** 5828
Fogler M M 2001 *Preprint* cond-mat/0107306
[17] Zhang F C and Das Sarma S 1986 *Phys. Rev.* B **33** 2903
[18] Metropolis N, Rosenbluth A W, Rosenbluth M N, Teller A M and Teller E 1953 *J. Chem. Phys.* **21** 1087
[19] Girvin S M, MacDonald A H and Platzman P M 1986 *Phys. Rev.* B **33** 2481
[20] Rezayi E and Read N 1994 *Phys. Rev. Lett.* **72** 900